

Supplementary Materials for

Structural basis for recognition of frizzled proteins by *Clostridium difficile* toxin B

Peng Chen^{1†}, Liang Tao^{2†}, Tianyu Wang¹, Jie Zhang², Aina He^{2,5}, Kwok-ho Lam¹, Zheng Liu¹,
Xi He³, Kay Perry⁴, Min Dong^{2*}, Rongsheng Jin^{1*}

Correspondence to: R.J. (r.jin@uci.edu), M.D. (min.dong@childrens.harvard.edu)

This PDF file includes:

Materials and Methods

Figs. S1 to S11

Tables S1 to S3

Materials and Methods

Cloning, expression, and purification of recombinant proteins

The gene encoding TcdB-FBD (residues 1285-1804) was cloned into a modified pET28a vector with a 6xHis-SUMO (*Saccharomyces cerevisiae* Smt3p) tag introduced to its N-terminus. A second TcdB-FBD construct was made by adding an additional HA tag to the C terminus, which was used for BLI, pull down, and cell surface binding assays. The CRD of human Frizzled 2 (residues 24-156) was cloned into a modified pcDNA vector for mammalian cell expression, and a human IL2 signal sequence (MYRMQLLSIALSLALVTNS), a 9xHis tag, and a human rhinovirus 3C protease cleavage site were added to its N-terminus. All mutated TcdB-FBD variants were generated by two-step PCR and verified by DNA sequencing.

TcdB-FBD was expressed in *E. coli* strain BL21-Star (DE3) (Invitrogen). Bacteria were cultured at 37°C in LB medium containing kanamycin. The temperature was reduced to 16°C when OD₆₀₀ reached ~0.8. Expression was induced with 1 mM IPTG (isopropyl-b-D-thiogalactopyranoside) and continued at 16°C overnight. The cells were harvested by centrifugation and stored at -80°C until use.

TcdB-FBD and its variants were purified using Ni²⁺-NTA (nitrilotriacetic acid, Qiagen) affinity resins in a buffer containing 50 mM Tris, pH 8.0, 400 mM NaCl, and 40 mM imidazole. The proteins were eluted with a high-imidazole buffer (50 mM Tris, pH 8.0, 400 mM NaCl, and 300 mM imidazole) and then dialyzed at 4°C against a buffer containing 20 mM HEPES, pH 7.5, and 150 mM NaCl. After cleaving the His-SUMO tag by SUMO protease, TcdB-FBD and its variants were further purified by MonoQ ion-exchange (20 mM Tris, pH 8.5) and Superdex-200 size-exclusion chromatography (GE Healthcare, 20 mM Tris, pH 8.0, and 100 mM NaCl).

CRD2 was expressed and secreted from FreeStyle HEK 293 cells (ThermoFisher) and purified directly from cell culture medium using Ni²⁺-NTA resins. The TcdB-FBD-CRD2 complex was prepared by mixing the purified TcdB-FBD and CRD2 at a molar ratio of ~1:3 for 2 hours on ice, and the complex was further purified using a MonoQ ion-exchange column (20 mM Tris, pH 8.5). The complex was concentrated to ~10 mg/ml for crystallization. The purity of the TcdB-FBD, TcdB-FBD-HA, and His-CRD2 is shown in fig. S9.

Crystallization

Initial crystallization screens were carried out at 20°C using a Gryphon crystallization robot (Art Robbins Instruments) with high-throughput crystallization screening kits (Hampton Research and Qiagen). The best crystals of TcdB-FBD-CRD2 complex suitable for X-ray diffraction were obtained using hanging-drop vapor diffusion in a reservoir containing 0.1 M sodium acetate (pH 5.0) and 1 M ammonium sulfate. For cryo-protection, the reservoir solution was supplemented with additional 2.2 M sodium malonate. Crystals of the platinum-derived TcdB-FBD-CRD2 complex were obtained by soaking native crystals in 100 mM potassium tetracyanoplatinate (II) for 5 minutes and cryoprotected similarly as native crystals.

Data collection and structure determination

The X-ray diffraction data were collected at 100 K at the NE-CAT beamline 24-ID-C, Advanced Photon Source (APS). The data were processed with XDS as implemented in RAPD (<https://github.com/RAPD/RAPD>) (31). For the Pt-soaked TcdB-FBD-CRD2 complex, 0.2

degree, 0.2 second exposure fine phi-sliced data using a PILATUS 6MF was collected at the Platinum LIII peak above the absorption edge (1.0717 Å) using one crystal. A native 2.5 Å dataset was collected using 0.2 degree, 0.2 second exposure at 0.9791 Å wavelength using one crystal. The single wavelength anomalous dispersion dataset of the TcdB-FBD-CRD2 complex was sufficient to calculate the initial phase using PHENIX.AutoSol (32). The phase information was used to build an initial model using PHENIX.AutoBuild (32), which was improved through multiple cycles of manual model building in COOT (33) and refinement in Phenix (32). This partially refined structure was then used as a search model in molecular replacement on the native 2.5 Å dataset using PHENIX.Phaser (32). Further structural modeling and refinement were carried out iteratively using COOT (33) and Phenix.Refinement (32). All the refinement progress was monitored with the free R value using a 5% randomly selected test set (34). The structure was validated through MolProbity (35). Data collection and structural refinement statistics are listed in Table S2. All structure figures were prepared with Pymol (DeLano Scientific).

Protein melting assay

The thermal stability of TcdB-FBD variants was measured using a fluorescence-based thermal shift assay on a StepOne real-time PCR machine (Life Technologies). Each protein (~0.1 mg/ml) was mixed with the fluorescent dye SYPRO Orange (Sigma-Aldrich) and heated from 25°C to 95°C in a linear ramp. The midpoint of the protein-melting curve (T_m) was determined using the analysis software provided by the instrument manufacturer. Data obtained from three independent experiments were averaged to generate the bar graph.

Cell lines, antibodies and constructs

HeLa (H1, #CRL-1958), 293T (#CRL-3216), L cells (#CRL-2648), and L/Wnt3A (#CRL-2647) cells were originally obtained from ATCC. They tested negative for mycoplasma contamination, but have not been authenticated. HeLa-Cas9, HeLa-Cas9 *FZD1/2/7*^{-/-}, and HeLa-Cas9 *CSPG4*^{-/-} cells were generated in-house and have been described previously (13). Stable HeLa-FZD7^{CRD}-Myc-GPI cells were generated by lentiviral transduction of HeLa H1 cells with a construct expressing FZD7^{CRD}-Myc-GPI (pLEX_307 vector, #41392, Addgene), followed by selection with 5 µg/ml puromycin. The following mouse monoclonal antibodies were purchased from the indicated vendors: 1D4 tag (MA1-722, ThermoFisher Scientific), HA tag (16B12, Covance), β-actin (AC-15, Sigma), Myc tag (9E10, ThermoFisher Scientific). Rabbit monoclonal antibodies against DVL2 (30D2, #3224) and Wnt3a (#2391) was purchased from Cell Signaling. Rabbit polyclonal antibody against Claudin-3 (ab15102) was purchased from Abcam. Chicken polyclonal IgY (#754A) against TcdB was purchased from List Biological Labs. Antibody validation is available on the manufacturers' websites. pRK5-FZD2-1D4 was originally generated in J. Nathans' laboratory (Baltimore, MD) and were obtained from Addgene (#42254). Full-length FZD2-1D4 mutants were generated from pRK5-FZD2-1D4 by site-directed mutagenesis (Agilent Technologies, CA).

TcdB, Frizzled and other recombinant proteins

Recombinant full length TcdB (from *C. difficile* strain VPI 10463) was expressed in *Bacillus megaterium* as previously described (13, 36) and purified as a 6xHis-tagged protein. The purity of TcdB and TcdB^{GFE} is shown in fig. S9. Recombinant human proteins were purchased from

R&D Systems (FZD2^{CRD}-Fc, FZD8^{CRD}-Fc, and FZD9^{CRD}-Fc), Sino Biologicals (FZD4^{CRD}-Fc and FZD5^{CRD}-Fc), and StemRD (Wnt3A).

TcdB binding to cells and immunoblot analysis

Transient transfection of HeLa cells was carried out using PolyJet (SignaGen). Binding of TcdB to cells was analysed by exposing cells to TcdB (10 nM) or HA-tagged TcdB-FBD (100 nM) for 10 minutes at room temperature. Cells were washed three times with PBS and then harvested with RIPA buffer (50 mM Tris, 1% NP40, 150 mM NaCl, 0.5% sodium deoxycholate, 0.1% SDS, plus a protease inhibitor cocktail (Sigma-Aldrich)). Cell lysates were centrifuged and supernatants were subjected to SDS-PAGE and immunoblot analysis. Cell surface proteins biotinylation and isolation were carried out using PierceTM Cell surface Protein Isolation Kit (#89881, ThermoFisher Scientific) following the manufacturer's instruction. The original uncropped images of western blots are shown in figs. S10 and S11.

Cytopathic assay

The cytopathic effect (cell rounding) of TcdB was analysed using standard cell-rounding assay. Briefly, cells were exposed to a gradient of TcdB and TcdB^{GFE} for 24 hours. Phase-contrast images of cells were taken (Olympus IX51, ×10-20 objectives). The numbers of round shaped and normal shaped cells were counted manually. The percentage of round shaped cells was plotted and fitted using the Origin software. CR₅₀ is defined as the toxin concentration that induces 50% of cells to become round in 24 hours.

Pull-down assays

The pull-down assays between His-tagged CRD2 and TcdB-FBD variants were performed using Ni²⁺-NTA resins in 1 ml binding buffer containing 50 mM Tris, pH 8.5, 400 mM NaCl, 10 mM imidazole, and 0.1% Tween-20. His-tagged CRD2 served as the bait and TcdB-FBD variants (WT and mutants) were the preys. CRD2 was pre-incubated with Ni²⁺-NTA resins at room temperature for 30 minutes, and the unbound protein was washed away using the binding buffer. The resins were then divided into small aliquots and mixed with TcdB-FBD variants (~1.5 μM, ~2.5-fold molar excess over CRD2). Pull-down assays were carried out at room temperature for 30 minutes. The resins were then washed twice, and the bound proteins were released from the resins with 400 mM imidazole.

For the assays between FZD5^{CRD} and TcdB-FBD, 100 ng of FZD5^{CRD}-Fc protein premixed with or without 100 ng Wnt3A was immobilized on 30 μl of Protein G agarose beads (#20398, ThermoFisher Scientific) by incubation for 30 minutes at 4°C followed by washing with PBS. TcdB-FBD diluted in the indicated buffer was added and incubated for 30 minutes at 4°C. The beads were then washed, pelleted, boiled in SDS sample buffer, and subjected to immunoblot analysis. The palmitoleic acid (#P9417, Sigma-Aldrich) saturated PBS was generated as described previously (22). Briefly, 100 μl of palmitoleic acid stock (10 mg/ml in DMSO) was added into 10 ml of PBS, followed by incubation at room temperature with vigorous vortex for 2 hours. Palmitoleic acid suspension was then centrifuged at 14,000 rpm for 20 minutes, and the central part was taken as saturated buffer. DMSO was kept constant at 1% in both palmitoleic acid saturated and the control buffer.

Bio-layer interferometry (BLI) assays

The binding affinities between TcdB-FBD variants and FZD2^{CRD} were measured by BLI assay using the Blitz system (ForteBio). Briefly, FZD2^{CRD}-Fc (20 µg/ml) were immobilized onto capture biosensors (Dip and Read Anti-hIgG-Fc, ForteBio) and balanced with PBS. The biosensors were then exposed to different concentrations of TcdB-FBD or its mutants, followed by the dissociation in PBS. Binding affinities (K_D) were calculated using the Blitz system software (ForteBio). To analyze binding of TcdB to CRD-Wnt complex, Fc-tagged CRDs of FZD5, 4, 8, and 9 (20 µg/ml) were pre-mixed with or without Wnt3A (20 µg/ml) and incubated on ice for 30 minutes. The proteins were then immobilized onto capture biosensors and balanced with PBS. 5 µM TcdB-FBD or 1 µM TcdB were then applied to the loaded biosensors, followed by wash with PBS. To analyze sequential binding of Wnt3A and TcdB to CRD2, FZD2^{CRD}-Fc (20 µg/ml) were immobilized onto capture biosensors and balanced with PBS. The loaded biosensors were first exposed to 20 µg/ml Wnt3A, balanced again with PBS, and then exposed to 5 µM TcdB-FBD or 1 µM TcdB. Alternatively, the biosensors were first exposed to 5 µM TcdB-FBD or 1 µM TcdB, balanced with PBS, and then exposed to 20 µg/ml Wnt3A. All biosensors were then washed with PBS for the dissociation.

Wnt signalling assay

The TOPFLASH/TK-Renilla dual luciferase reporter assay was used to detect Wnt signalling. Briefly, HeLa or 293T cells in 24-well plates were co-transfected with TOPFLASH (50 ng/well), TK-Renilla (internal control, 10 ng/well), and pcDNA3 (200 ng/well). Wnt3A conditional medium (CM) was generated from L/Wnt3a cell cultures. Culture medium from L cells served as the control medium. After 24 hours, cells were exposed to either Wnt3A CM or control medium with or without TcdB-FBD (200 nM, unless otherwise noted) for 6 hours. Cell lysates were harvested and subjected to either Firefly/Renilla dual luciferase assay or immunoblot analysis for detecting phosphorylated DVL2. Wnt signalling activates expression of TOPFLASH luciferase reporter (firefly luciferase). Co-transfected Renilla luciferase serves as an internal control. The ability of FZD2^{K127A/E} to mediate Wnt signalling was examined using FZD1/2/7 KO HeLa cells, by co-transfection of TOPFLASH (100 ng/well), TK-Renilla (internal control, 20 ng/well), and WT or FZD2 mutants (500 ng/well). After 24 hours, cells were exposed to either Wnt3A CM or control medium for additional 6 hours. Cell lysates were harvested and subjected to either Firefly/Renilla dual luciferase assay or immunoblot analysis for detecting phosphorylated DVL2.

Cecum toxin injection assay

Mice (CD1, 6-8 weeks, both male and female, from Envigo) were anesthetized following overnight fasting. A midline laparotomy was performed to locate the cecum. 100 µl of saline, TcdB or TcdB^{GFE} (15 µg) was injected into the connection part between ileum and cecum via insulin syringe (29G1/2), followed by closing the wounds with stitches. Mice were allowed to recover and euthanized 12 hours later to harvest the cecum tissue. We noted that some mice died within a few hours after the surgery (<5 hours, 4 of 10 for TcdB and 3 of 10 for TcdB^{GFE}), which were not included in the subsequent study (28). The cecum tissues were then fixed, paraffin-embedded, sectioned, and subjected to either hematoxylin and eosin (H&E) staining for histological score analysis or immunofluorescent staining for Claudin-3.

Histological analysis and immunofluorescence staining

The cecum tissues were washed with PBS for three times, followed by fixing in 10% phosphate buffered formalin for 24 hours. The tissues were embedded in paraffin and sectioned 5 µm each.

Histology analysis was carried out with H&E staining. Stained sections were scored by observers blinded to experimental groups, based on 4 criteria including disruption of the epithelia, hemorrhagic congestion, mucosal edema, and inflammatory cell infiltration, on a scale of 0 to 3 (normal, mild, moderate, or severe). Immunofluorescence analysis of Claudin-3 was carried out using rabbit anti-Claudin-3 (1:100) polyclonal antibody. Confocal images were captured with the Ultraview Vox Spinning Disk Confocal System.

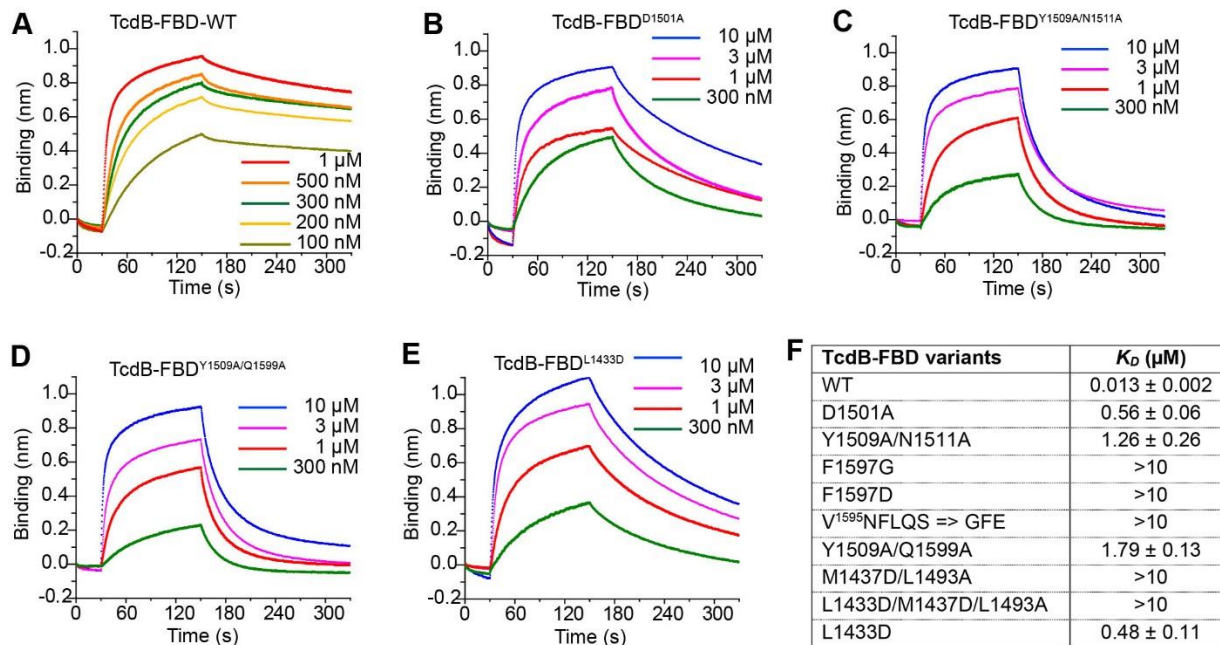


Fig. S1. Binding of TcdB-FBD variants to CRD2. Representative binding curves of TcdB-FBD variants to recombinant Fc-tagged CRD2 examined by BLI assays. (A) WT TcdB-FBD bound to CRD2 with a high affinity. Four TcdB-FBD variants tested in this study displayed significantly weakened binding to CRD2: TcdB-FBD-D1501A (B), TcdB-FBD-Y1509A/N1511A (C), TcdB-FBD-Y1509A/Q1599A (D), and TcdB-FBD-L1433D (E). All other variants tested did not show detectable binding to CRD2. The concentrations of TcdB-FBD variants were labeled in each panel. Binding analysis results are summarized in (F). Shown values are means \pm s.d. of three experiments.

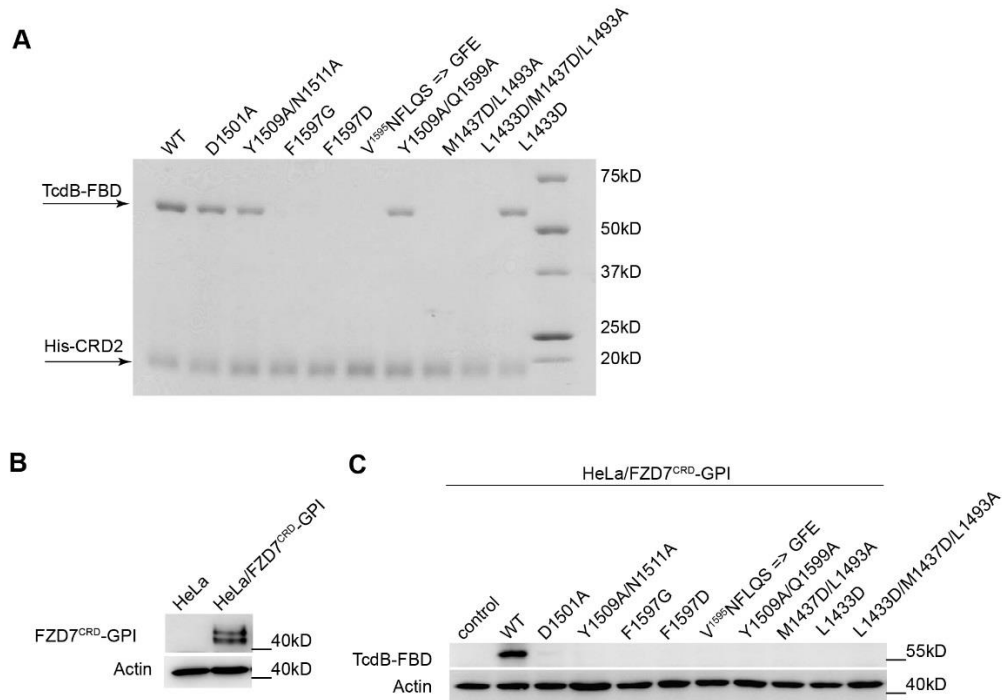


Fig. S3. Characterization of the binding of TcdB-FBD variants to His-tagged CRD2 or FZD7^{CRD}-GPI on cell surface. (A) Binding of TcdB-FBD variants (~1.5 μ M) to the immobilized His-tagged CRD2 was examined using pull-down assays. Samples were analyzed by SDS-PAGE and Coomassie Blue staining. (B) FZD7^{CRD}-Myc-GPI was stably expressed in the HeLa/ FZD7^{CRD}-GPI cell line as detected by the anti-Myc antibody. (C) TcdB-FBD mutants (~50 nM) failed to bind HeLa/ FZD7^{CRD}-GPI cells when compared to WT TcdB-FBD. Cell lysates were harvested and subjected to immunoblot analysis.

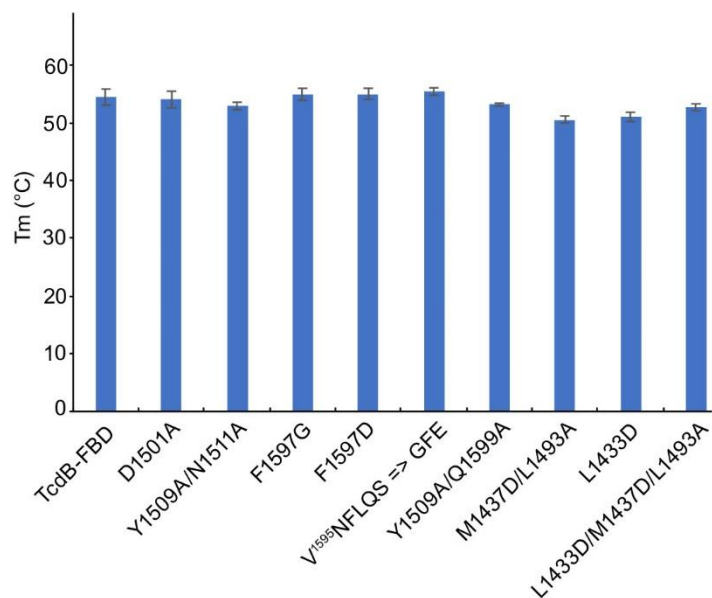


Fig. S4. TcdB-FBD variants adopt wild-type-like structures. The thermal stability of proteins was measured using a fluorescence-based thermal shift assay on a StepOne real-time PCR system (ThermoFisher). Protein melting was monitored using a hydrophobic dye, SYPRO Orange (Sigma-Aldrich), as the temperature was increased in a linear ramp from 25°C to 95°C. The midpoint of the protein-melting curve (T_m) was determined using the software provided by the instrument manufacturer. The data are presented as mean \pm s.d. ($n = 3$). All the TcdB-FBD variants showed T_m values comparable to the wild-type protein, indicating correct protein folding.

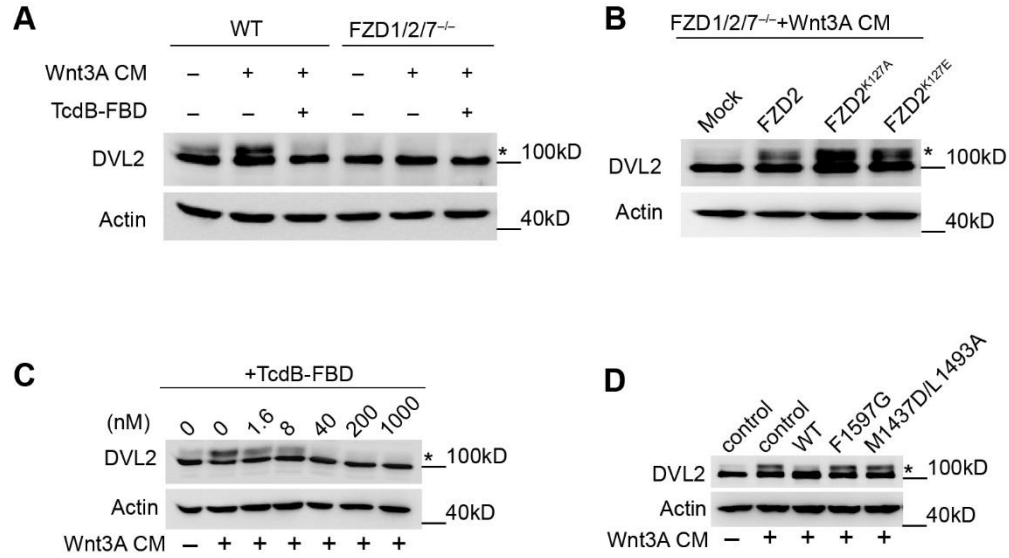


Fig. S5. Characterization of the selected TcdB-FBD and FZD2 mutants by measuring Wnt-induced DVL2 phosphorylation. (A) DVL2 phosphorylation induced by Wnt3A CM in WT and FZD1/2/7 triple KO HeLa cells. Asteroids (*) indicate the phosphorylated DVL2. (B) DVL2 phosphorylation induced by Wnt3A CM in FZD1/2/7 triple KO cells expressing WT FZD2 or the K127A/E mutants. (C) TcdB-FBD (40 nM) was able to inhibit the phosphorylation of DVL2 induced by Wnt3A CM in HEK293T cells. (D) Wnt-induced DVL2 phosphorylation was inhibited by WT TcdB-FBD, but not the F1597G or M1437D/L1493A mutants.

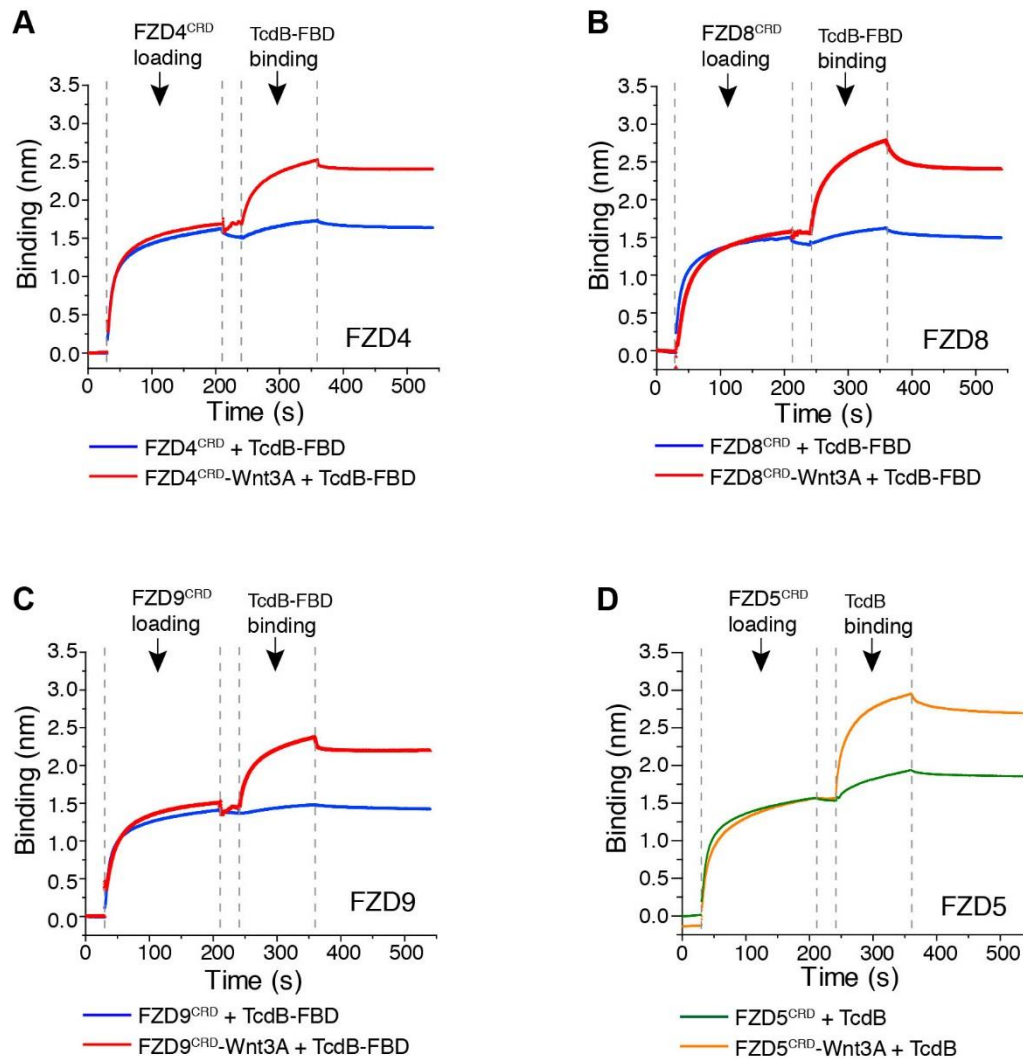


Fig. S6. Pre-loading Wnt3A enhanced binding of TcdB to various CRDs. Binding of TcdB-FBD to CRDs of FZD4 (A), FZD8 (B), and FZD9 (C) was enhanced by pre-loading Wnt3A to CRDs in BLI assays. CRDs-Fc and Wnt3A were pre-mixed and loaded to the biosensor, followed by sequential exposure to 5 μ M TcdB-FBD. (D) Binding of full-length TcdB to CRD5 was enhanced by pre-loading Wnt3A to CRD5 in BLI assays. CRD5-Fc and Wnt3A were pre-mixed and loaded to the biosensor, followed by sequential exposure to 1 μ M TcdB.

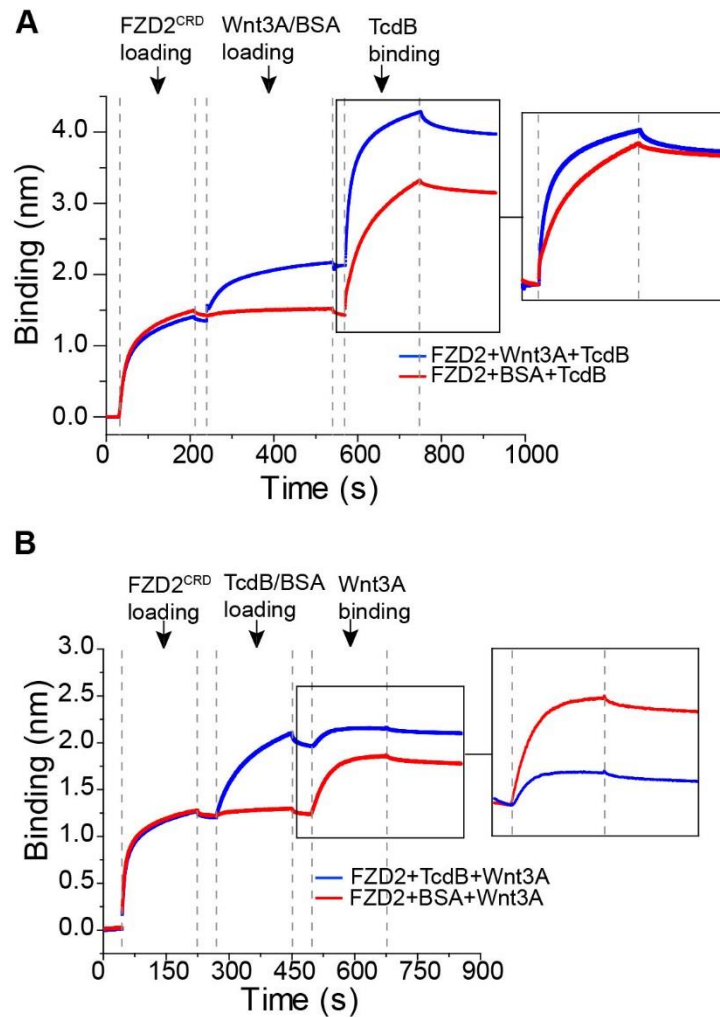


Fig. S7. Wnt3A did not affect the binding of full-length TcdB to CRD2, but TcdB impeded binding of Wnt3A to CRD2. The relationship between Wnt3A and full-length TcdB in terms of their binding to CRD2 was accessed via sequential protein loading in BLI assays. Binding of full-length TcdB to CRD2 was marginally changed when CRD2 was pre-bound with Wnt3A (**A**). In contrast, binding of TcdB to CRD2 blocked subsequent binding of Wnt3A (**B**). BSA (0.1 mg/ml) served as a control. Different loading steps are noted.

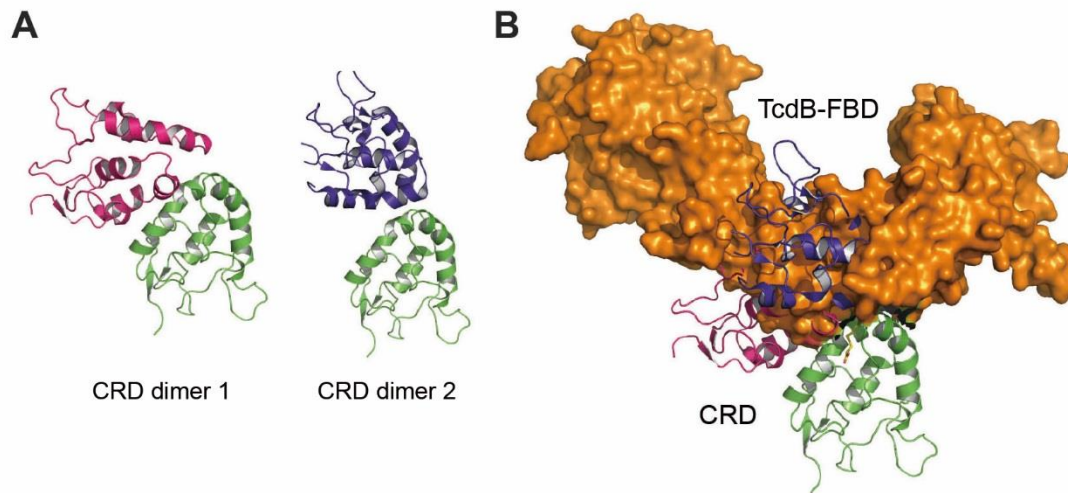


Fig. S8. TcdB blocks CRD dimerization. (A) Two different configurations of CRD dimers (red-green and blue-green) are proposed to be involved in Wnt activation (22, 27). (B) These two proposed CRD dimer assemblies are superimposed to the TcdB-FBD-CRD2 complex. Both are incompatible with the TcdB-FBD-CRD2 complex due to steric competition.

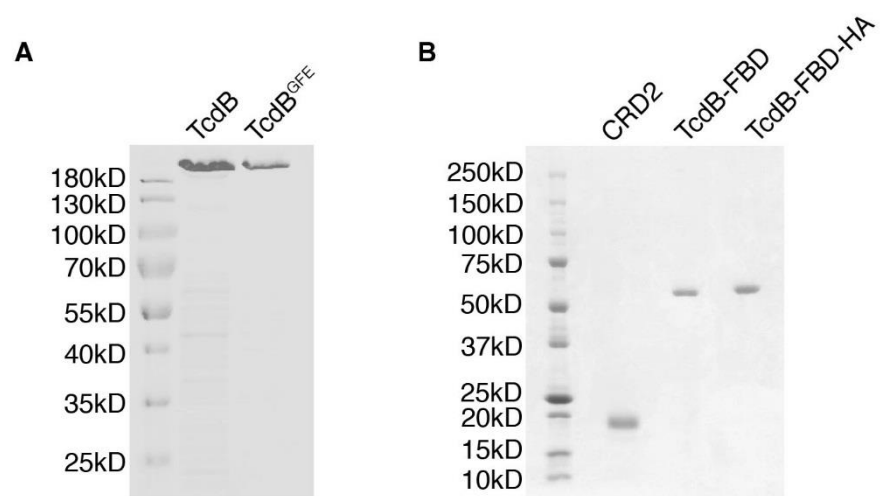


Fig. S9. The purity of (A) TcdB and TcdB^{GFE} and (B) His-CRD2, TcdB-FBD, and TcdB-FBD-HA were analyzed by SDS-PAGE and Coomassie Blue staining.

Figure 3A

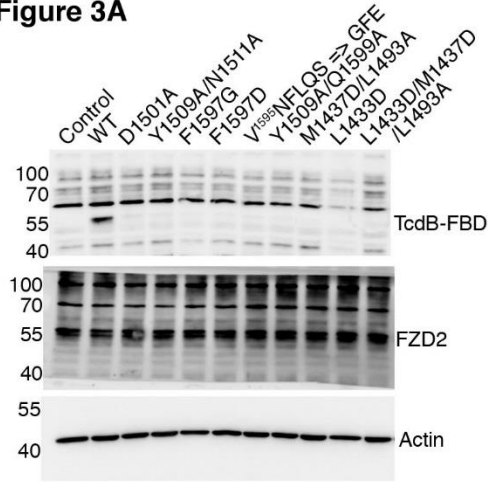


Figure 3C

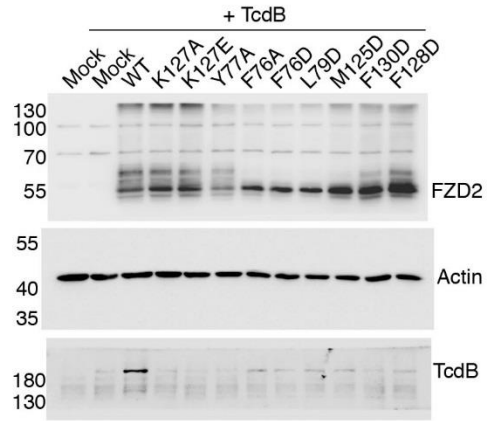


Figure 3D

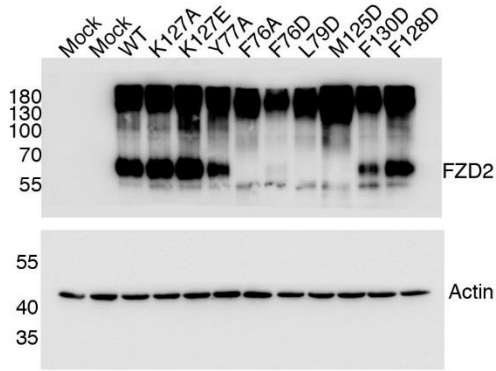


Figure 4C

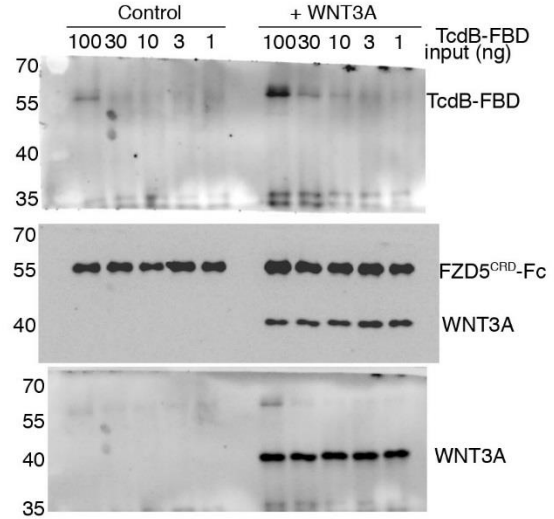


Figure 4A

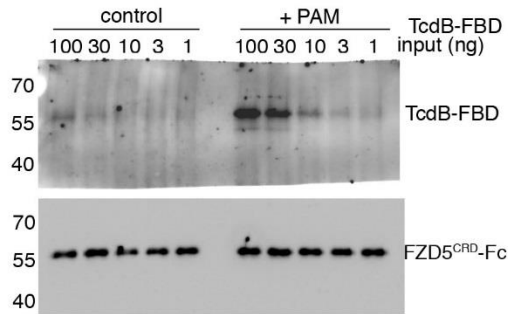


Fig. S10. Original uncropped images of western blots shown in Fig. 3 and Fig. 4

Figure S3B

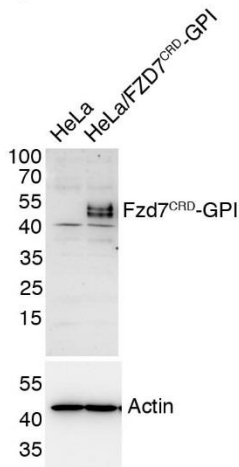


Figure S3C

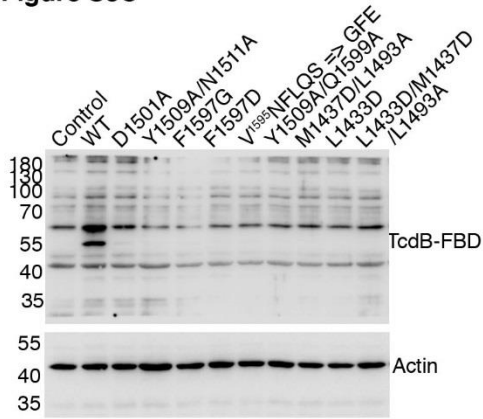


Figure S5A

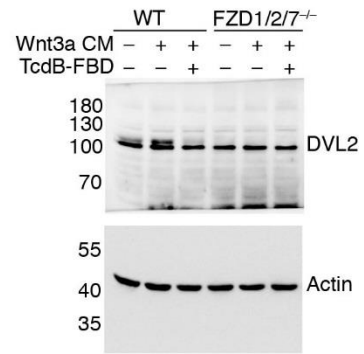


Figure S5B

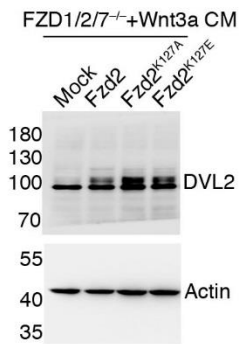


Figure S5C

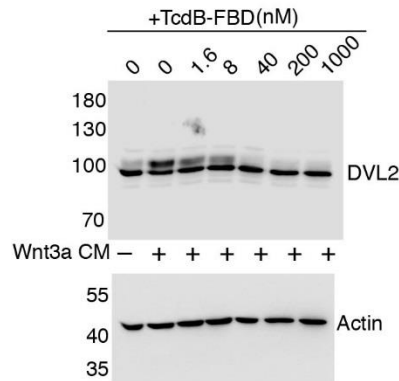


Figure S5D

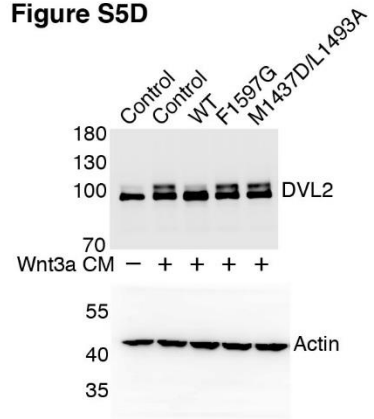


Fig. S11. Original uncropped images of western blots shown in Figs. S3 and S5.

Table S1. Characterization of various TcdB truncations.

Fragment boundaries	Expression	Biochemical behavior *	Pull down by His-CRD2
792-1835	Yes	Low purity, aggregated	N/A
1024-1804	Yes	Monodispersed	Yes
1028-1835	Yes	Monodispersed	Yes
1071-1512	Yes	Monodispersed	No
1114-1835	Yes	Monodispersed	Yes
1114-2101	Yes	Monodispersed	Yes
1133-1835	Yes	Low purity, aggregated	N/A
1285-1608	No	N/A	N/A
1285-1640	No	N/A	N/A
1285-1660	No	N/A	N/A
1285-1804 (TcdB-FBD)	Yes	Monodispersed	Yes
1294-1835	Yes	Low purity, aggregated	N/A
1313-1616	No	N/A	N/A
1340-1616	No	N/A	N/A
1365-1804	Yes	Low purity, aggregated	N/A
1394-1835	Yes	Low purity, aggregated	N/A
1400-1804	Yes	Low purity, aggregated	N/A
1401-1835	Yes	Low purity, aggregated	N/A
1430-1804	Yes	Monodispersed	No
1454-1804	Yes	Monodispersed	No
1501-1835	Yes	Low purity, aggregated	N/A
1501-2366	Yes	Monodispersed	No
1510-1688	Yes	Monodispersed	No
1510-1804	Yes	Monodispersed	No
1688-1835	Yes	Monodispersed	No

* The aggregation state of the proteins was judged based on Superdex-200 size-exclusion chromatography.

Table S2. Data collection, phasing, and refinement statistics

	Native	Pt-SAD
Data collection		
Space group	C222 ₁	C222 ₁
Cell dimensions		
<i>a, b, c</i> (Å)	74.6, 175.6, 174.4	73.3, 177.1, 174.6
α, β, γ (°)	90, 90, 90	90, 90, 90
Wavelength (Å)	0.9791	1.0717
Resolution (Å)	87.86 - 2.50 (2.56 - 2.50) *	88.56 - 2.72 (2.82 - 2.72) *
<i>R</i> _{merge} (%) ^a	4.68 (59.5)	9.64 (>100)
<i>R</i> _{pim} ^b	0.03 (0.35)	0.04 (0.76)
Wilson <i>B</i> -factor (Å ²)	56	68
<i>I</i> / σI	18.3 (1.8)	15.7 (1.0)
<i>CC</i> _{1/2} ^c	0.999 (0.849)	0.999 (0.778)
Completeness (%)	98.2 (99.0)	93.4 (80.3)
Redundancy	3.7 (3.6)	6.5 (6.3)
Refinement		
Resolution (Å)	87.81 - 2.50 (2.90 - 2.50) *	
No. reflections	39,324	
<i>R</i> _{work} ^d / <i>R</i> _{free} ^e	19.87/23.74	
No. atoms		
Protein	4,978	
Ligand/ion	53	
Water	37	
<i>B</i> -factors (Å ²)		
Protein	74	
Ligand/ion	99	
Water	68	
Ramachandran plot		
Favored (%)	94.5	
Allowed (%)	5.5	
Outliers (%)	0.0	
R.m.s deviations		
Bond lengths (Å)	0.008	
Bond angles (°)	1.030	

* Values in parentheses are for the highest-resolution shell.

^a $R_{\text{merge}} = \frac{\sum hkl \sum i |I_i - \langle I \rangle|}{\sum hkl \sum i I_i}$, where I_i is the intensity of the i th observation, $\langle I \rangle$ is the mean intensity of the reflection and the summations extend over all unique reflections (hkl) and all equivalents (i), respectively.

^b $R_{\text{pim}} = \frac{\sum hkl [n/(n-1)]^{1/2} \sum i |I_i(hkl) - \langle I(hkl) \rangle|}{\sum hkl \sum i I_i(hkl)}$, where n is the multiplicity, other variables as defined for R_{merge} .

^c $CC_{1/2}$ = Pearson correlation coefficient between random half-datasets.

^d $R_{\text{work}} = \frac{\sum h |F_o(h) - |F_c(h)||}{\sum h |F_o(h)|}$, where $|F_o|$ and $|F_c|$ are the observed and calculated structure-factor amplitudes, respectively.

^e R_{free} was calculated with 5% of the data excluded from the refinement.

Each dataset was derived from a single crystal.

Table S3. Protein-protein and protein-lipid interactions in the TcdB-FBD-CRD2 complex.Protein-protein contacts between TcdB-FBD and CRD2

CRD2 residues	TcdB-FBD residues	Type of interaction
H74	Y1509 Q1599	Hydrogen bond (sc-sc) Hydrogen bond (sc-sc)
Q75	F1597	Hydrogen bond (sc-mc)
Y77	V1491 Y1509 N1511	vdW (sc-sc) vdW (sc-sc) Hydrogen bond (sc-sc)
P78	L1493 F1597 Y1509	vdW (sc-sc) vdW (sc-sc) vdW (sc-sc)
K81	L1488 D1490	vdW (mc-sc) Salt bridge (sc-sc)
V82	K1434 L1493	Hydrogen bond (mc-sc) vdW (sc-sc)
Q83	K1434 E1468	Hydrogen bond (mc-sc) Hydrogen bond (sc-sc)
A123	L1438	vdW (sc-sc)
L124	M1437 L1438	vdW (sc-sc) vdW (sc-sc)
K127	M1437 D1501 S1505	Hydrogen bond (sc-mc) Salt bridge (sc-sc) Hydrogen bond (mc-mc)
F128	M1437 S1495 V1497 S1505 S1505 F1597	vdW (sc-sc) vdW (sc-sc) vdW (sc-sc) vdW (sc-sc) Hydrogen bond (mc-mc) vdW (sc-sc)
F130	L1598	vdW (sc-sc)

PAM-mediated interactions between TcdB-FBD and CRD2

	CRD2/TcdB residues	Type of interaction
PAM-CRD2	Q75 F76 P78 L79 V82 V124 M125 F128 F130	vdW vdW vdW vdW vdW vdW vdW vdW vdW
PAM-TcdB-FBD	L1433 M1437 S1486 L1493 S1495 F1597	vdW vdW vdW vdW vdW vdW

“vdW” stands for van der Waals interaction.

“mc” and “sc” indicates whether the contact is mediated by main-chain or side-chain atoms.